

Evolution of coherent dark states

L. Liu,¹ M. J. Bellanca,² and H. Metcalf¹

¹*Physics and Astronomy, State University of New York, Stony Brook, New York 11794-3800*

²*Faculty of Physics, M696, University of Konstanz, 78457 Konstanz, Germany*

(Received 28 September 2001; published 7 March 2002)

We present a set of exploratory experimental studies of velocity-selective coherent population trapping (VSCPT) on the $2^3S_1 \rightarrow 2^3P_1$ transition of Helium, including the effect of an external magnetic field along the propagation direction of the light. We also investigate in detail the effects of the laser detuning and the atom-laser interaction time in determining the shape and width of the VSCPT velocity distribution. Our data corroborates some previous theory and calculations. We demonstrate that the only observable effect of a magnetic field applied along the direction of light propagation is to shift the center of the VSCPT peaks in the atomic velocity distribution by an amount proportional to the magnitude of the applied field. We present a semiclassical picture that describes the atomic motion of VSCPT in such a B field.

DOI: 10.1103/PhysRevA.65.043401

PACS number(s): 32.80.Pj, 42.50.Vk

I. INTRODUCTION

Interference effects created by the superposition of wave amplitudes are manifest throughout physics. Perhaps the most familiar is the intensity modulation of light in interferometers, but also well known is the interference of quantum-mechanical transition amplitudes [1–3]. When an interference phenomenon is described by variables of more than one distinct Hilbert space, conflicts often arise between our intuitive picture of the classical world and its correct quantum-mechanical description. If one of these Hilbert spaces is macroscopic, such as motion, and the superposition produces entanglement of the variables, then *welcher weg* questions arise, such as the Einstein-Podolsky-Rosen paradox and many other “puzzles” of quantum physics.

The interference of quantum-mechanical transition amplitudes is well established [1–3]. One recent example of such interference, combined with the entanglement of variables from two disparate Hilbert spaces, is velocity-selective coherent population trapping (VSCPT), first described in 1988 [4,5].

VSCPT is most easily understood for a two-level atom moving in one dimension (1D) in a monochromatic, standing-wave light field [6,7]. The light field couples pairs of degenerate motional states of opposite momenta (and thus the same kinetic energy). The optical coupling is represented by off-diagonal elements in the atom-light Hamiltonian matrix that result in new, nondegenerate eigenstates. One of these is a superposition of ground atomic states for which the interference of transition amplitudes nearly isolates it from the light field. This light-decoupled state is called a “dark state.”

In the original one-dimensional VSCPT experiment [4,5], the presence of multiple atomic levels resulted in an entanglement of internal atomic states with external motional states of the atoms, and the optical polarization selection rules were exploited to produce a completely dark state. When a dark state is also an eigenstate of the complete Hamiltonian that includes the center-of-mass momentum, atoms accumulate in this state and are trapped. Thus the stable atomic ground states critically define the external motional

state, and the atomic sample can become extremely “cold” [8].

In this paper we discuss some of our recent studies of VSCPT. We investigate the effect of an external magnetic field along the propagation direction of the light field, and we present a semiclassical picture that describes the atomic motion. We examine in detail the effects of the laser parameters and the atom-laser interaction time in establishing the characteristic double-peaked feature in the velocity distribution of atoms trapped in the dark state of VSCPT. We present our data that corroborates the theory and calculations of Ref. [9]. We demonstrate experimentally the capability to tune the center of the characteristic double-peaked velocity distribution $\mathcal{N}(v)$ of VSCPT and to choose laser parameters where $\mathcal{N}(v)$ can be a single peak with subrecoil width.

II. VSCPT IN A MAGNETIC FIELD

A. Intuitive energy considerations

VSCPT requires optical coupling between distinct momentum states $|1\rangle$ and $|2\rangle$ of ground-state atoms, and momentum conservation requires that these states be separated by $\pm 2n\hbar\vec{k}$, where \vec{k} is the wave vector of magnitude $2\pi/\lambda$, and n is an integer that will be unity hereafter. The resulting coupled state is stationary only if its components are degenerate, and in the two-level atom case, this simply requires $p_1^2/2M = p_2^2/2M$ (M is the atomic mass). Thus the center-of-mass momenta of the coupled states must be $\pm\hbar\vec{k}$. The presence of an applied magnetic field has no effect on the momenta [6].

By contrast, in a real atom with multiple ground-state sublevels, the presence of a magnetic field can split the energies of the components of the ground-state superposition. Then the degeneracy condition becomes

$$p_1^2/2M + g_J\mu_B M_1 B = p_2^2/2M + g_J\mu_B M_2 B, \quad (1)$$

where g_J is the Landé g factor, μ_B is the Bohr magneton, and the M_i 's are the magnetic quantum numbers of the relevant ground-state sublevels.

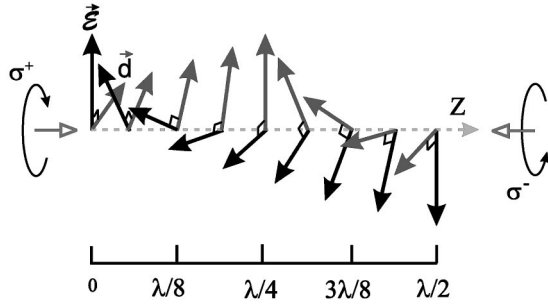


FIG. 1. A semiclassical picture of the condition $\vec{d} \cdot \vec{E} = 0$. The optical field is produced by counterpropagating, oppositely circularly polarized light beams, and the result is a helical \vec{E} field [10,11]. The atomic dipole moment, here labeled \vec{d} , precesses about the \hat{z} axis at the Larmor frequency, and the atomic velocity $v = \omega_Z/k$ synchronizes this precession with motion in the helical field so that the two vectors remain perpendicular.

For the most well-studied example of VSCPT, the atomic transition is $J=1 \rightarrow 1$, and the light field has counterpropagating beams of oppositely circularly polarized light [4,5,8]. When the \hat{z} axis and \vec{B} field are chosen along the \vec{k} vector of one of the light beams, the selection rules require that the light can only couple the ground states $M_J = \pm 1$, and Eq. (1) is satisfied for

$$\bar{v} = -\omega_Z/k. \quad (2)$$

Here $\omega_Z = g_J \mu_B M_J B / \hbar$ is the Zeeman frequency shift of the M_J state, $g_J = 2$ for this 2^3S state, and $\bar{v} = (p_1 + p_2)/2M$.

In some sense, \bar{v} is the average velocity of a single atom whose motional components have two different velocities. This may seem counterintuitive from a classical perspective in which a massive atom should have only one velocity. That is, we tend to think that there must exist a rest frame for such a massive particle. In VSCPT each atom is in a superposition of motional states, and no such rest frame exists.

B. Semiclassical model

There is a very appealing semiclassical model that also leads to Eq. (2). In order for a ground state $|g\rangle$ to be dark, the off-diagonal Hamiltonian matrix element $\mathcal{H}_{eg} = \vec{E} \cdot \langle e | \vec{d} | g \rangle$ must vanish. Here $|e\rangle$ is the excited state and both the electric dipole and rotating wave approximations have been made. Since neither the optical electric field \vec{E} nor the atomic electric dipole moment $\langle e | \vec{d} | g \rangle$ is zero, \mathcal{H}_{eg} can only vanish when $\vec{d} \perp \vec{E}$.

For the VSCPT $J=1 \rightarrow 1$ case under consideration here, the electric field of counterpropagating circularly polarized light beams is linearly polarized everywhere, but not in a fixed direction [10,11]. The polarization and maximum field value trace a helical path of pitch λ along the \hat{z} axis as shown in Fig. 1. In order to maintain the condition $\vec{d} \perp \vec{E}$, the dipole moment of an atom moving at velocity v must rotate about \hat{z} at frequency $\omega = 2\pi v/\lambda = kv$.

The classical response of a magnetic dipole moment $\vec{\mu}$ in an applied magnetic field \vec{B} is precession, and for the case of an atom, the precession frequency is $\omega_Z = g \mu_B B / \hbar$. Thus atoms precessing at ω_Z will maintain their orientation perpendicular to \vec{E} if their velocity satisfies Eq. (2), as shown in Fig. 1.

This picture can be pushed a little in the quantum-mechanical domain by considering that the external momentum of the states is determined so that the atoms must be spatially delocalized. Thus the wave function must have a helical geometry oriented to satisfy $\vec{d} \perp \vec{E}$. In the laboratory frame, this wave packet moving at velocity \bar{v} “snakes” along the helical \vec{E} field, and we have dubbed this picture the “Larmor snake.”

Of course, for the atoms in the subrecoil VSCPT peaks, a semiclassical model is suspect. Atoms in this trapped state can be thought of as two delocalized traveling de Broglie waves moving in opposite directions with de Broglie wavelength equal to that of the light. Clearly these atoms are far from the semiclassical regime, where they can be pictured as localizable particles. This fundamentally quantum-mechanical superposition state is deeply within the quantum regime where classical analogies often break down.

C. Hamiltonian and wave functions

The discussion above can be described more formally by specifying a basis set and considering the total Hamiltonian. There are three basis sets to consider: (1) the “atomic” basis, whose elements are specified by the familiar atomic quantum numbers; (2) the “optical” basis, usually considered in most descriptions of VSCPT, where the ground states of the atomic basis are combined into a new orthonormal set according to their optical coupling via Raman transitions [4,5,8]; and (3) the “total” basis, comprised of eigenstates of a total Hamiltonian that includes both the atomic kinetic energy and the Zeeman effect [9,12]. We discuss mainly the third of these, and will begin with the magnetic field $B=0$, which corresponds to the case of Ref. [9].

For the $J=1 \rightarrow 1$ level scheme and counterpropagating oppositely circularly polarized light beams, optical pumping quickly depopulates the “atomic” ground-state sublevel with $M_J=0$, as well as the excited states with $M_J = \pm 1$ [5]. Thus there remains a “ Λ ” system of three “atomic” levels coupled by the light field. Including the external motion results in a closed momentum family whose ground states are $|++\rangle \equiv |M_J=+1, \mathcal{P}=p+\hbar k\rangle$ and $|--\rangle \equiv |M_J=-1, \mathcal{P}=p-\hbar k\rangle$ where \mathcal{P} is the center-of-mass momentum of each component state. The excited state of this Λ system has $M_J=0$ and momentum $\mathcal{P}=p$, and is written as $|0,p\rangle$. The ground states are most naturally rearranged into a new basis set [9,5,13]

$$|NC\rangle = \frac{|++\rangle + |--\rangle}{\sqrt{2}} \quad \text{and} \quad |C\rangle = \frac{|++\rangle - |--\rangle}{\sqrt{2}}. \quad (3)$$

Thus $|NC\rangle$ (noncoupled) and $|C\rangle$ (coupled) are superposi-

tions of states of different external momenta, and it is this superposition that results in the classically puzzling VSCPT state discussed at the end of Sec. II A.

The four terms of the total Hamiltonian are

$$\mathcal{H} = \mathcal{H}_{atom} + \mathcal{H}_Z + \mathcal{H}_{KE} + \mathcal{H}_{int}. \quad (4)$$

In the bare atomic state basis, \mathcal{H}_{atom} simply provides the energy of the excited state $|0, p\rangle$, and \mathcal{H}_Z is the Zeeman term whose eigenvalues are $\pm \hbar \omega_Z$ (\pm because $M_J = \pm 1$). Also, the eigenvalues of the kinetic-energy term \mathcal{H}_{KE} are given by $\mathcal{P}^2/2M$. Finally, \mathcal{H}_{int} is the interaction between the light field and the atom, and so $\mathcal{H}_{int}|NC\rangle = 0$ [7,5].

Application of the total Hamiltonian of Eq. (4) to $|NC\rangle$, and rearrangement of the terms leads to

$$\mathcal{H}|NC\rangle = \frac{p^2 + (\hbar k)^2}{2M}|NC\rangle - \hbar \left(\frac{kp}{M} + \omega_Z \right) |C\rangle. \quad (5)$$

For $\omega_Z = 0$ ($B = 0$) we recover the familiar case of VSCPT where $|NC\rangle$ is indeed a trapped state (eigenstate) for $p = 0$. Any value of $p \neq 0$ results in a nondiagonal Hamiltonian matrix whose eigenstates are, therefore, a mixture of $|NC\rangle$ and $|C\rangle$ (see Sec. III A below). When the mixing term $\hbar kp/M$ is small [14], the eigenstate closest to $|NC\rangle$ is still weakly coupled, and often denoted $|WC\rangle$. Similarly, the state nearest $|C\rangle$ is still strongly coupled and denoted $|SC\rangle$. The state $|WC\rangle$ may be excited and the subsequent decay may leave it in $|NC\rangle$ at $p = 0$. A detailed calculation of the mixing coefficients of the eigenstates is in Ref. [9], but is outlined in Sec. III A below.

For $B \neq 0$, Eq. (5) shows that $|NC\rangle$ is an eigenstate of the total Hamiltonian of Eq. (4) only for $p = -M\omega_Z/k$. This is exactly the condition of Eq. (2) since the average velocity of the components of $|NC\rangle$ is $\bar{v} = p/M$. Thus we expect the average velocity of atoms in $|NC\rangle$ to shift from $\bar{v} = 0$ with applied magnetic field [15]. This is related to velocity selective resonance (VSR) [16] and will be discussed more thoroughly in a subsequent paper [17].

Just as the transformation of Eq. (3) for the internal states provides a clearer description of the interaction between the atoms and the light field for the $B = 0$ case, a transformation of the external coordinates to a frame moving at velocity $\bar{v} = v_{VSR} = p_{VSR}/M = \omega_Z/k$ leads to a cleaner description of the atomic motion for $B \neq 0$.

Following Ref. [12], we simply replace \mathcal{P} by $\mathcal{P} - p_{VSR}$ in the definitions of $|++\rangle$ and $|--\rangle$, and find that the components of the transformed states $|NC\rangle$ and $|C\rangle$ acquire a phase $\pm kv_{VSR}t$. The new eigenstates are straightforward to calculate and are the same as $|C\rangle$ and $|NC\rangle$, except for $\mathcal{P} \rightarrow \mathcal{P} - p_{VSR}$.

D. Experimental results

1. Apparatus

Our atomic beam and laser setup have been described previously [6,12,18] but are summarized here. A beam of metastable He (He*) atoms in the 2^3S state of about

10^{14} atoms/s sr, is generated in a dc discharge followed by a set of apertures. The atoms have an average velocity of ~ 1100 m/s and a spread of about $\pm \sim 200$ m/s. The longitudinal velocity distribution was measured by time of flight that was implemented by chopping the atomic beam. Atoms enter an interaction region where the magnetic field is controlled by three small pairs of perpendicular Helmholtz coils to $\pm 5-10$ μ T.

Here they cross a 22-mm-wide laser field of counter-propagating, circularly polarized, $\lambda = 1.083$ μ m light from a diode laser. The laser frequency is locked by saturated absorption spectroscopy to the He* resonance line using an *rf* discharge in a static cell. The saturated absorption signal from the cell is collision broadened to about 15 MHz, nearly ten times the natural width of the $2^3S \rightarrow 2^3P$ of interest here. The laser can be readily tuned to excite the $J = 0, 1$, or 2 sublevel of the 2^3P state.

Next the atoms fly freely for 1.4 m where they impinge on a detector mounted behind a 30- μ m slit. Atoms that pass through the slit impinge on a stainless plate where their 20 eV of internal energy releases an electron. The electrons are attracted to a multichannel plate multiplier by a bias voltage, and its output signal is further amplified and recorded as a computer-controlled stepping motor scans the entire detector assembly across the atomic beam profile. From this measure of the 1D spatial profile of the beam, the transverse velocity distribution of the atoms resulting from their interaction with the transverse laser beam is inferred.

2. Data

The state $|NC\rangle$ is decoupled from the laser light by virtue of the interference of the excitation amplitudes [4,5,8]. It is an eigenstate of the total Hamiltonian, and thus it is stationary if the second term of Eq. (5) vanishes. We, therefore, expect the characteristic two-peaked signal of VSCPT to shift from $\bar{v} = 0$ to $\bar{v} = \omega_Z/k$ as the applied field $\vec{B} = B_z \hat{z}$ is varied. The positive \hat{z} direction is defined by the helicity of the optical standing wave. (The case of \vec{B} not along the optical \vec{k} vectors will be addressed in a later paper [17].)

A small sample of a large data set is shown in Fig. 2. For this data set, the laser frequency was detuned $\delta \equiv \omega_{laser} - \omega_{atom} \cong -0.5\gamma \cong 2\pi \times 800$ kHz below atomic resonance. Here $\gamma = 1/\tau$ is the natural width of the excited state, and the average intensity I in the quasi-Gaussian beam profile was $I \cong 0.18$ mW/cm² $\cong 1.1 \times I_{sat}$ ($I_{sat} \equiv \pi \hbar c / 3\lambda^3 \tau \approx 160$ μ W/cm² for the transition used here). Each curve results from a single scan, and the total acquisition time is about 3 min. If the centers of these signals are plotted against B_z the resulting straight line has slope and intercept compatible with $\bar{v} = \omega_Z/k$ and our calibration of the coils.

Similar experiments have been done on the $2^3S \rightarrow 3^3P$ at $\lambda = 389$ nm [6,19]. The near-uv light is produced by frequency doubling light from a Ti:sapphire laser using an external buildup cavity. For these uv experiments a different detection scheme was employed. The He* atoms impinge on a multichannel plate and their 20 eV of internal energy causes the release of electrons. The subsequently amplified

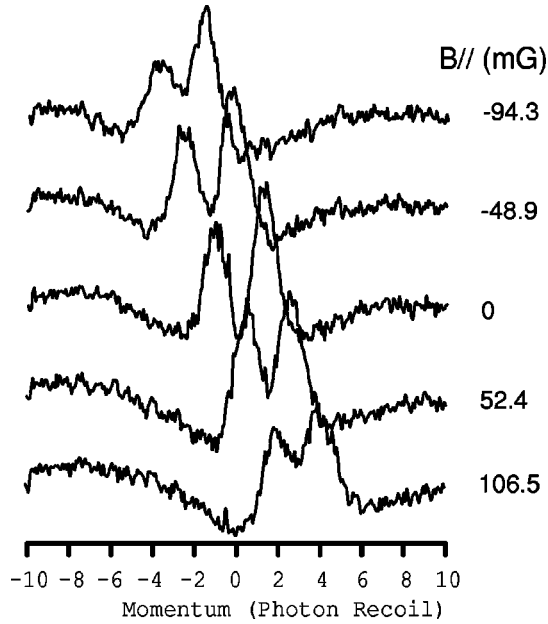


FIG. 2. VSCPT signals taken from Fig. 4.17 of Ref. [12]. The saturation parameter is $s=1.1$ and the detuning was $\delta \approx -0.5\gamma$. This is part of a data set with about 20 such traces, and a plot of the center position of the two peaks vs $|\vec{B}|=B_z$ is a straight line with slope consistent with $v = \omega_z/k$. The two peaks are superposed on a baseline that dips to a minimum between them, and so each peak sits on a baseline sloping upwards away from the center. Thus they are shifted apart by several percent of their widths, so their separation is about 4% larger than two recoils. This dip is the combination of the residual dip that occurs for VSCPT with $\delta < 0$ in a finite interaction time and the trapping of atoms from the neighborhood of momentum space into the VSCPT peaks.

electron shower is accelerated to a phosphor screen and a visible image is formed. This image is captured by a charge-coupled device camera outside the vacuum system and is recorded using a PC with a frame grabber card. We average across the image to determine the atomic distribution and from this we extract the velocity distribution. The data have similar signal-to-noise ratio as that of the infrared light data, but each curve results from a single frame, and so the acquisition time is only 1/30 s. The field dependence of the position of the signals is also compatible with $\bar{v} = \omega_z/k$ and our calibration of the coils.

3. Uncertainties

There are only small errors associated with these measurements. The transverse velocity calibration is determined by the longitudinal velocity and the geometry, and is corroborated by the separation between the peaks. The trajectory of the atoms through the field and the laser beams is not exactly determined, leaving some residual uncertainties about the field magnitude experienced by the atoms. The longitudinal velocity spread of the beam broadens the peaks by about 20%, but the dominant source of their width is the limited cooling during the finite interaction time as they cross the laser field.

The largest uncertainty of a few percent arises from the calibration between the coil current and field. One source of error is the Hall probe meter itself, and another is the field inhomogeneity that is measurable (few percent). The inhomogeneities in the magnetic field produce small (on the order of a few microtesla) fields in the two directions perpendicular to \hat{z} . These fields cause a mixing of the magnetic sublevels caused by Larmor precession. For our experiment, though, the Larmor precession time for these fields between two sublevels is several times the interaction time, and its effects can be safely neglected.

It is important to realize that the case for a magnetic field parallel to the \vec{k} vector of the light field does not differ substantially from the $B=0$ VSCPT case, except for the velocity at which the double peaks are centered. In terms of the peak development, effects of interaction time, light intensity, and detuning, the two cases are identical, as discussed below. Mathematically, we can see the two cases as a simple linear transformation in momentum. Experimentally, we see parallel results as the light parameters and interaction time are tuned.

III. ESTABLISHING VSCPT

A. The $p \neq 0$ case

For $|\vec{B}|=0$ and $q \equiv p/\hbar k \neq 0$, $|NC\rangle$ and $|C\rangle$ are not eigenfunctions of \mathcal{H} as shown by Eq. (5). The off-diagonal terms $\langle C|\mathcal{H}|NC\rangle$ then lead to new eigenvalues $E_{SC,WC}$ given in Ref. [9] as

$$E_{SC,WC}/E_r = u + q^2 + 1 \pm X, \quad X \equiv \sqrt{u^2 + 4q^2}, \quad (6)$$

where the “+ (–)” sign is for SC (WC), the “strongly (weakly) coupled” state [20]. We have defined $E_r \equiv (\hbar k)^2/2M$, $s \equiv I/I_{sat}$, and $u \equiv s\hbar\delta/\{4E_r[1 + (2\delta/\gamma)^2]\}$. For $q=0$, $E_{WC}=E_{NC}=E_r$ since the only nonzero energy term is kinetic, deriving from the mixture of wave function components with momenta $= \pm \hbar k$ (the dark state wave function $|NC\rangle$ has no interaction with the laser light).

Likewise, the eigenfunctions are no longer $|C\rangle$ and $|NC\rangle$, but are q -dependent mixtures, also given in Ref. [9] as

$$|SC\rangle(|WC\rangle) = \alpha_{\pm}|NC\rangle + \beta_{\pm}|C\rangle, \quad (7)$$

with

$$|\alpha_{\pm}|^2 = \frac{(-u + 2q \pm X)^2}{2[u^2 + (2q \pm X)^2]} = 1 - |\beta_{\pm}|^2. \quad (8)$$

As above, for $q=0$ we recover the eigenstates $|C\rangle$ and $|NC\rangle$.

As for the $p=0$ case, transformation to a frame moving at $v = v_{VSR}$ is both helpful and straightforward. Again, following Ref. [12], we simply replace \mathcal{P} by $\mathcal{P} - p_{VSR}$. The new eigenstates are straightforward to calculate, and can be readily expanded in terms of $|C\rangle$ and $|NC\rangle$ with the same results as in Eqs. (7) and (8), except for $\mathcal{P} \rightarrow \mathcal{P} - p_{VSR}$ and $p \rightarrow p - p_{VSR}$.

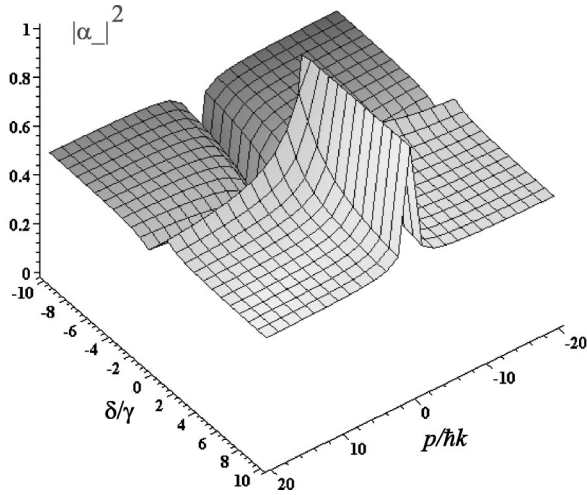


FIG. 3. Plot of $|\alpha_-|^2$ vs momentum and detuning taken from Fig. 3.2 of Ref. [12]. The nearly plane areas that occupy most of the parameter space correspond to $|\alpha_-|^2 \approx 1/2$ for which the eigenstates are nearly equal mixtures of $|NC\rangle$ and $|C\rangle$. Thus the basis set $|C\rangle$ and $|NC\rangle$ is a good choice only in the regions where the momentum is small and $|\alpha_-|^2 \approx 1$ or $|\alpha_-|^2 \ll 1$, depending on the sign of δ .

B. Evolution of the two-peaked velocity distribution

Until now, the discussion has focused on the steady-state two-peaked velocity distribution $\mathcal{N}(v)$ of atoms in $|NC\rangle$ for $q=0$ (or in $|WC\rangle$ for $|q|<1$). This may be appropriate after many optical pumping cycles, but not after only a few. Figure 3 shows that $0.4 < |\alpha_-|^2 < 0.6$ for almost all detunings and momenta except for a narrow channel near $p=0$ (slightly wider near $\delta=0$). This means that, over most of parameter space, the system's eigenstates are not well described by $|C\rangle$ and $|NC\rangle$, and furthermore that such atoms are readily excited. Atoms having $|q|>1$ do not contribute to the VSCPT signals.

For $|q|<1$, there are two time scales to consider. The faster one is the optical pumping rate for atoms in $|SC\rangle$ given by Ref. [7],

$$\gamma_p \equiv \frac{s\gamma/2}{1 + s + (2\delta/\gamma)^2}. \quad (9)$$

For most of our data, $|\delta| \sim \gamma$ and $s \sim 1$ so $\gamma_p \sim \gamma/12$, corresponding to an optical pumping time of $\sim 12\tau \sim 1.2 \mu\text{s}$. Thus most atoms in $|SC\rangle$ have undergone several optical pumping cycles during the first $\sim 10 \mu\text{s}$ of interaction with the laser light. We can safely assume that their velocity distribution is then relatively flat, or its population has been pumped to very high values of \bar{v} so it contributes little to our signal.

By contrast, the slow time scale of optical pumping for atoms in $|WC\rangle$ is determined by the small fraction $\beta_-|C\rangle$ that is mixed into $|WC\rangle$ [see Eq. (7) and Fig. 3] [21]. For typical parameters of $\delta = \gamma$ and $s = 1$, Eq. (8) gives $|\alpha_-|^2 = 0.95$ so $\beta_- = 0.22$ in the region of $|q| \sim 1/2$. The pumping time for atoms in $|WC\rangle$ becomes more than $5 \mu\text{s}$, so there is only time for ~ 2 optical pumping cycles in the first $\sim 10 \mu\text{s}$

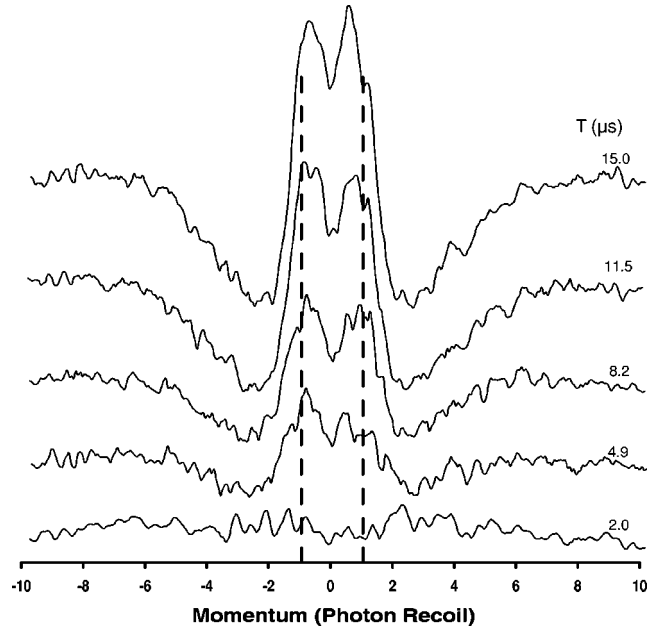


FIG. 4. Plots of VSCPT signals obtained with various interaction times, taken from Fig. 4.15 of Ref. [12]. For these data the saturation parameter $s \approx 0.66$ and the detuning $\delta \approx +0.62\gamma$. Thus $\gamma_p \approx \gamma/5$ and $\beta_- \approx 0.3$ (for $q=0.5$) so the optical pumping time is $\approx \tau/0.06 \approx 1.7 \mu\text{s}$. The double-peaked structure just begins to emerge after $4.9 \mu\text{s}$, but is clear after $8.2 \mu\text{s}$, suggesting that at least three optical pumping cycles are needed for their unambiguous visibility. The two peaks are superposed on a baseline that dips in the neighborhood of $|q|>3$ because of the capture of atoms into the VSCPT peaks, as in Fig. 2, but also has a strong local maximum in the neighborhood of $|q|<1$ because $\delta > 0$. The dominant effect is to move the peaks closer together by several percent of their widths.

of interaction with the laser light. Therefore the transient population of atoms in $|WC\rangle$ needs to be considered carefully.

As shown in Ref. [9], the population remaining in $|WC\rangle$ in states having $|q| \sim 1/2$ after only a few optical pumping cycles has a very strong effect on the total $\mathcal{N}(v)$. The short-term result for $\mathcal{N}(v)$ is a single narrow peak or dip, depending on the sign of δ . This peak is more “square” than a Gaussian, has a FWHM of $\sim 2v_r = 2\hbar k/M$, and, therefore, an rms width of less than v_r . We have found that it is ubiquitous in laser-cooling experiments [17]. Both an initial peak ($\delta > 0$) and a dip ($\delta < 0$) evolve into the two-peaked velocity distribution after 3 or 4 optical pumping cycles, which corresponds to our full $20 \mu\text{s}$ interaction time for typical laser parameters.

C. Experimental results

Figure 4 shows a series of our measurements of VSCPT signals taken with $\delta = 0.62\gamma$, $s = 0.66$, and $B = 0$. The interaction time was varied by changing the width of the laser beam crossed by the atoms with an adjustable aperture. It very nearly reproduces the behavior in Fig. 6(d) of Ref. [9].

Consider a state $|WC\rangle$ evaluated at $q = 1/2$. For these parameters, Eq. (8) gives $\beta_- \sim 1/3$, Eq. (9) yields $\gamma_p \approx \gamma/10$,

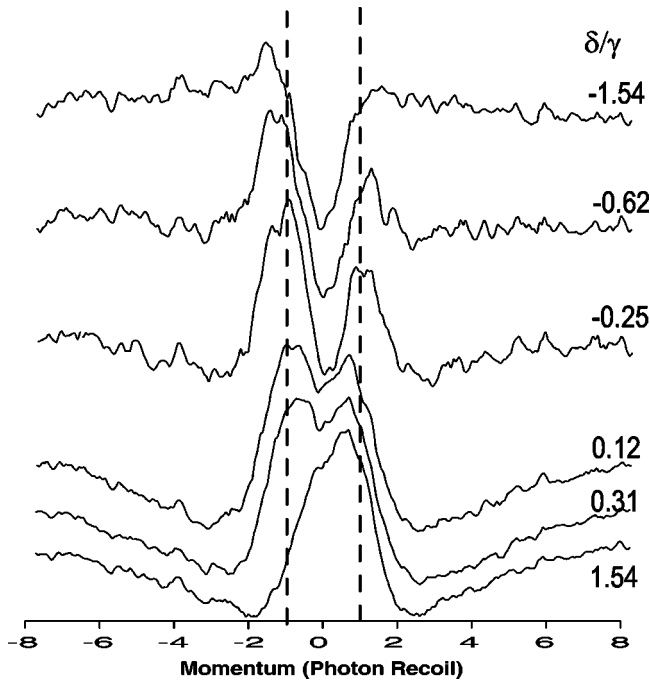


FIG. 5. Plots of VSCPT signals obtained at various detunings, taken from Fig. 4.12 of Ref. [12]. For these data the saturation parameter $s \approx 1.32$ and the interaction time was the full $20 \mu s$. At large detunings there is clearly only a single peak or dip, whereas the familiar double-peaked signal is clear at small detunings, especially for $\delta < 0$. This is the region where γ_p is large enough to allow several optical pumping cycles during the interaction time. The effects of the time-dependent residual peak or dip that depends on the sign of δ is clear in these data. The peaks for $\delta < 0$ are much more widely spaced than those for $\delta > 0$.

and so an optical pumping cycle takes about 30τ or $\sim 3 \mu s$. Then Fig. 4 shows that two or three optical pumping cycles are sufficient to produce visible twin peaks in $\mathcal{N}(v)$, completely consistent with the calculations shown in Fig. 6(d) of Ref. [9].

Figure 5 presents a series of our measurements of VSCPT signals taken with the full $20 \mu s \sim 200\tau$ interaction time at $s = 1.32$ and $B = 0$. The detuning is varied over a range that is $\approx 3\gamma$. The signals clearly show the single narrow peak and

dip at the detuning extremes, as predicted in Ref. [9]. In addition, for $|\delta| \sim 1.5$, we find $\gamma_p \sim \gamma/18$ from Eq. (9), and so there is time for only ~ 2 optical pumping cycles of $|WC\rangle$. Correspondingly, the twin peaks are not noticeable. By contrast, for smaller $|\delta|$, γ_p is significantly larger and the peaks are well formed. Note that the depth of the dip between the peaks is much greater for $\delta < 0$ than for $\delta > 0$, also as predicted in Ref. [9].

IV. CONCLUSIONS AND OUTLOOK

We have extended the study of one-dimensional VSCPT into two new domains of parameters: applied magnetic field and optical excitation. In the case of $\vec{B} = B_z$ where the \hat{z} axis is defined by the \vec{k} vector of one of the light beams, we have shown that there is no change in the nature of VSCPT. Instead, the position of the characteristic two-peaked signal merely shifts from being centered at $v = 0$ to $v = \omega_z/k$. We have shown how this result can be calculated analytically from a Hamiltonian that contains the center-of-mass motion of the atoms. We have also provided a semiclassical description of this effect.

We have also studied VSCPT signals produced by changing the laser parameters and interaction time, and we have found results consistent with Ref. [9]. Moreover, we have measured the evolution from the single, subrecoil-width velocity distribution to the familiar double-peaked distribution of VSCPT as the laser parameters vary, and also as the interaction time varies. We suggest that these results are connected by the limited number of optical pumping cycles in each case.

We plan to apply these ideas to the case of “leaky” dark states, i.e., those states for which the departure rate from $|WC\rangle$ is determined either by a weak excitation or by a mixing process. We have already explored some leaky dark states in Ref. [6], but are now investigating the idea for applications to VSR experiments. Previous VSR experiments have shown tantalizingly narrow signals [22,23] whose widths defy explanation in terms of optical cooling. These narrow velocity distributions may arise precisely from the optical pumping mechanism presented here.

[1] E. Arimondo and G. Orriols, *Lett. Nuovo Cimento Soc. Ital. Fis.* **17**, 33 (1976).
 [2] H.M. Gray, R. Whitley, and C. Stroud, *Opt. Lett.* **3**, 218 (1978).
 [3] W.A. Davis, W.D. Phillips, and H. Metcalf, *Phys. Rev. A* **19**, 700 (1979).
 [4] A. Aspect, E. Arimondo, R. Kaiser, N. van Steenkiste, and C. Cohen-Tannoudji, *Phys. Rev. Lett.* **61**, 826 (1988).
 [5] A. Aspect, E. Arimondo, R. Kaiser, N. van Steenkiste, and C. Cohen-Tannoudji, *J. Opt. Soc. Am. B* **6**, 2112 (1989).
 [6] J. Hack, L. Liu, M. Olshanii, and H. Metcalf, *Phys. Rev. A* **62**, 013405 (2000).
 [7] H. Metcalf and P. van der Straten, *Laser Cooling and Trapping*

(Springer Verlag, New York, 1999).

[8] C. Cohen-Tannoudji, in *Laser Manipulation of Atoms and Ions*, Proceedings of the International School of Physics “Enrico Fermi,” Course CXVIII, edited by E. Arimondo, W. D. Phillips, and F. Strumia (North-Holland, Amsterdam, 1992), p. 99.
 [9] M. Doery, M. Widmer, M.-J. Bellanca, W. Buell, T. Bergeman, H. Metcalf, and E.J.D. Vredenburg, *Phys. Rev. A* **52**, 2295 (1995).
 [10] A. Kastler, *C. R. Acad. Sci. Paris* **271**, 999 (1970).
 [11] J. Dalibard and C. Cohen-Tannoudji, *J. Opt. Soc. Am. B* **6**, 2023 (1989).
 [12] Liang Liu, Ph.D. thesis, State University of New York, Stony Brook, 2001.

- [13] The state $|NC\rangle$ has a sum instead of a difference of its components because the Clebsch-Gordan coefficients for excitation of $|--\rangle$ and $|++\rangle$ have opposite signs.
- [14] Here, small means that the frequency $kp/M = \omega_D$, the Doppler shift, satisfies $\omega_D t_{int} \ll 1$, where t_{int} is the experimental interaction time. Thus “small” is an experimental condition.
- [15] J. Lawall, S. Kulin, B. Saubamea, N. Bigelow, M. Leduc, and C. Cohen-Tannoudji, *Laser Phys.* **6**, 153 (1996).
- [16] S.-Q. Shang, B. Sheehy, P. van der Straten, and H. Metcalf, *Phys. Rev. Lett.* **65**, 317 (1990).
- [17] M.-J. Bellanca *et al.* (unpublished).
- [18] M. Doery, M. Widmer, M.-J. Bellanca, E. Vredenburg, T. Bergeman, and H. Metcalf, *Phys. Rev. Lett.* **72**, 2546 (1994).
- [19] O. Kritisun, C. Affolderbach, and H. Metcalf, *Bull. Am. Phys. Soc.* **46**, 99 (2001), S5 20.
- [20] Since we consider a spread of momenta around $p=0$, the states of interest are $|WC\rangle$ and $|SC\rangle$ instead of simply $|NC\rangle$ and $|C\rangle$.
- [21] For $\delta < 0$, the roles of α and β are reversed.
- [22] M. Hoogerland, H. Beijerinck, K. van Leeuwen, P. van der Straten, and H. Metcalf, *Europhys. Lett.* **19**, 669 (1992).
- [23] M.-J. Bellanca, Ph.D. thesis, State University of New York, Stony Brook, 1999.